

Buckling Analysis of Curved Composite Sandwich Panels Subjected to Inplane Loadings

Juan R. Cruz
NASA Langley Research Center
Hampton, Virginia 23681

522-24

51422

Introduction

Composite sandwich structures are being considered for primary structure in aircraft such as subsonic and high speed civil transports. The response of sandwich structures must be understood and predictable to use such structures effectively. Buckling is one of the most important response mechanisms of sandwich structures. In reference 1, a simple buckling analysis is derived for sandwich structures. This analysis is limited to flat, rectangular sandwich panels loaded by uniaxial compression (N_x) and having simply supported edges. In most aerospace applications, however, the structure's geometry, boundary conditions, and loading are usually very complex. Thus, a general capability for analyzing the buckling behavior of sandwich structures is needed.

The present paper describes and evaluates an improved buckling analysis for cylindrically curved composite sandwich panels. This analysis includes orthotropic facesheets and first-order transverse shearing effects. Both simple support and clamped boundary conditions are also included in the analysis. The panels can be subjected to linearly varying normal loads N_x and N_y in addition to a constant shear load N_{xy} . The analysis is based on the modified Donnell's equations for shallow shells [2]. The governing equations are solved by direct application of Galerkin's method. The accuracy of the present analysis is verified by comparing results with those obtained from finite element analysis for a variety of geometries, loads, and boundary conditions. The limitations of the present analysis are investigated, in particular those related to the shallow shell assumptions in the governing equations. Finally, the computational efficiency of the present analysis is considered.

Panel Geometry

The geometry of the composite panel analyzed in this study is shown in figure 1. This panel is rectangular, of length a and width b . The panel is cylindrically curved with radius of curvature R . The panel as a whole, and the individual facesheets, are symmetrically laminated. In addition, the facesheets are considered to be specially orthotropic plates ($A_{16} = A_{26} = 0$, $D_{16} = D_{26} = 0$). The principal directions of the core material are assumed to coincide with the x and y coordinate directions. The core possesses only shear stiffness and is also considered to be specially orthotropic. Only two constants, G_{xz} and G_{yz} , are needed to define the core shear stiffness. Monolithic panels are a special case of the composite sandwich panel shown in figure 1. For monolithic panels the core thickness is zero and the total panel thickness is denoted by t_0 . The transverse shear moduli G_{xz} and G_{yz} are those of the panel material.

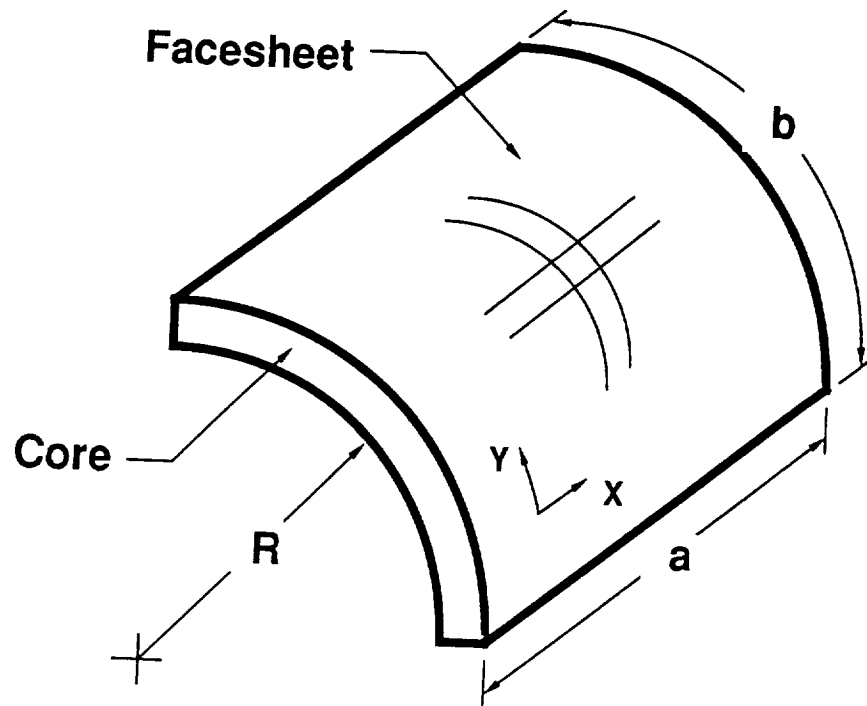


Figure 1

Panel Loading and Boundary Conditions

General inplane loadings, N_x , N_y , and N_{xy} are considered for the sandwich panels in this study. In the present study the panel can be subjected to linearly varying N_x and N_y loads, in addition to a constant N_{xy} load. An example loading is shown in figure 2. All four edges of the panel must have the same boundary condition and may be either simply supported or clamped.

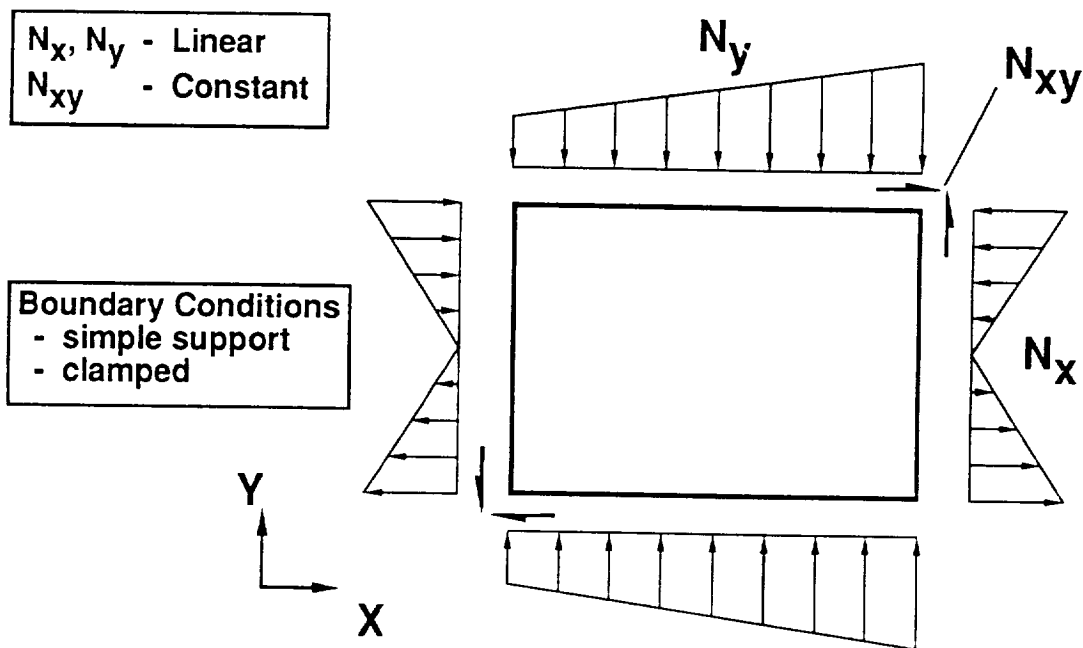


Figure 2

Governing Partial Differential Equations

The governing differential equations for buckling used in this study were derived in reference 2. These equations are three, coupled equations in the unknowns w , Q_x , and Q_y , the out-of-plane displacement and the transverse shear stress resultants, respectively. These equations form a set of Donnell's equations modified to include first order transverse shear effects.

An inverse differential operator is used with the governing equations to avoid escalating the partial differential equation. As shown in reference 3, escalating differential equations may lead to incorrect solutions. The inverse differential operator results when the inplane displacements u and v are removed as independent variables in the governing equations. A drawback of using this inverse differential operator is that boundary conditions cannot be specified for u and v ; these boundary conditions are implied in the assumed solution for w .

The governing equations used in the present study define a simple shell theory. The shell curvature, R , appears only in one term of the governing equations. In addition, an important simplifying assumption in the derivation of these equations is that the pre-buckling out-of-plane displacement w_0 can be ignored. These assumptions limit the application of these equations to shallow shells.

Assumed Series Solutions

The governing equations are solved using assumed trigonometric series for the independent variables w , Q_x , and Q_y . Two sets of series solutions corresponding to the simple support and the clamped boundary conditions are shown in figure 3. These series solutions must satisfy all boundary conditions. The series solution for w implies specific boundary conditions for u and v since an inverse differential operator is used to remove u and v as independent variables. Different boundary conditions for u and v than those implied by the series solution may result in significantly different buckling loads and mode shapes.

SIMPLY SUPPORTED SOLUTION

$$w = \sum_{m=1}^{\infty} \sum_{n=1}^{\infty} a_{mn} \sin\left(\frac{m\pi x}{a}\right) \sin\left(\frac{n\pi y}{b}\right)$$

$$Q_x = \sum_{m=1}^{\infty} \sum_{n=1}^{\infty} b_{mn} \cos\left(\frac{m\pi x}{a}\right) \sin\left(\frac{n\pi y}{b}\right)$$

$$Q_y = \sum_{m=1}^{\infty} \sum_{n=1}^{\infty} c_{mn} \sin\left(\frac{m\pi x}{a}\right) \cos\left(\frac{n\pi y}{b}\right)$$

CLAMPED SOLUTION

$$w = \sum_{m=1}^{\infty} \sum_{n=1}^{\infty} a_{mn} \left[\cos\left(m-1\right)\left(\frac{\pi x}{a}\right) - \cos\left(m+1\right)\left(\frac{\pi x}{a}\right) \right] \left[\cos\left(n-1\right)\left(\frac{\pi y}{b}\right) - \cos\left(n+1\right)\left(\frac{\pi y}{b}\right) \right]$$

$$Q_x = \sum_{m=1}^{\infty} \sum_{n=1}^{\infty} b_{mn} \left[\sin\left(m-1\right)\left(\frac{\pi x}{a}\right) - \sin\left(m+1\right)\left(\frac{\pi x}{a}\right) \right] \left[\cos\left(n-1\right)\left(\frac{\pi y}{b}\right) - \cos\left(n+1\right)\left(\frac{\pi y}{b}\right) \right]$$

$$Q_y = \sum_{m=1}^{\infty} \sum_{n=1}^{\infty} c_{mn} \left[\cos\left(m-1\right)\left(\frac{\pi x}{a}\right) - \cos\left(m+1\right)\left(\frac{\pi x}{a}\right) \right] \left[\sin\left(n-1\right)\left(\frac{\pi y}{b}\right) - \sin\left(n+1\right)\left(\frac{\pi y}{b}\right) \right]$$

Figure 3

Solution Approach

The governing equations are solved by Galerkin's method. Applying Galerkin's method as illustrated in figure 4 yields a set of equations which constitute a symmetric algebraic eigenvalue problem. Solving the eigenvalue problem yields the buckling loads and mode shapes.

Galerkin's Method

$$\int_0^a \int_0^b L_1(w, Q_x, Q_y) \left(\frac{\partial w}{\partial a_{mn}} \right) dy dx = 0$$

$$\int_0^a \int_0^b L_2(w, Q_x, Q_y) \left(\frac{\partial Q_x}{\partial b_{mn}} \right) dy dx = 0$$

$$\int_0^a \int_0^b L_3(w, Q_x, Q_y) \left(\frac{\partial Q_y}{\partial c_{mn}} \right) dy dx = 0$$

Figure 4

Analysis Verification

The present analysis has been implemented in two FORTRAN computer programs corresponding to the simple support and the clamped boundary conditions. The present analysis was verified and evaluated as outlined in figure 5. To verify the accuracy of the present analysis, comparisons are made with results obtained from a finite element analysis. In addition, the number of terms required in the solution series to achieve convergence is evaluated. Since the analysis is limited to shallow shells, the analysis accuracy is also assessed as a function of the panel curvature. Finally, the computational expense (as measured in CPU seconds) of the present method is compared to an equivalent solution obtained by a finite element analysis to assess the present method's computational efficiency.

- **Comparison with Finite Element results**
- **Convergence rate**
- **Limitations of shallow shell theory**
- **Computational efficiency**

Figure 5

Verification Test Cases

A set of 48 test cases has been defined and are described in figure 6. These test cases include a variety of geometries, materials, and loadings. For computational convenience, all test cases consist of monolithic panels. Transverse shear effects are introduced in some cases by setting low values for G_{xz} and G_{yz} . All panels are assumed to be made out of a typical graphite-epoxy composite material. The laminates are assumed to be homogeneous and to have either a unidirectional, with the 0° direction along the x axis, or a quasi-isotropic stacking sequence. Three sets of load conditions are considered: uniaxial compression only, shear only, and combined inplane bending and shear. All 48 test cases are evaluated for both simple support and clamped boundary conditions.

Wide range of test cases:

- **Geometry: length, width, radius of curvature**
- **Layup: isotropic, unidirectional**
- **Transverse shear stiffness: infinite, finite**
- **Loading: compression, shear, combined load**

Total load cases: 48

All test cases applied to both simply supported and clamped panels

Figure 6

Simply Supported Panels

Results for the buckling load ratio, R_s , as a function of the number of terms in the series solution are shown in figure 7 for plates with simple support boundary conditions. The buckling load ratio is defined as the ratio of the present analysis solution to the converged finite element solution. The finite element solution is assumed to be exact. Buckling load ratio results for the case with the worst convergence rate are shown by the solid line on the figure. Even for this worst case, ten terms for the assumed series solution were sufficient to obtain a converged R_s within one percent of the exact solution. Most other cases had converged results with much fewer terms for the assumed series solution. All 48 test cases converged to within ± 1 percent of the exact solution as illustrated by the dotted lines on the figure. These results illustrate that for panels consistent with the assumptions of the present analysis, accurate response can be predicted for a wide variety of structural parameters (e.g., high aspect ratio, high degree of orthotropy).

Convergence Rate and Comparison with FE Results

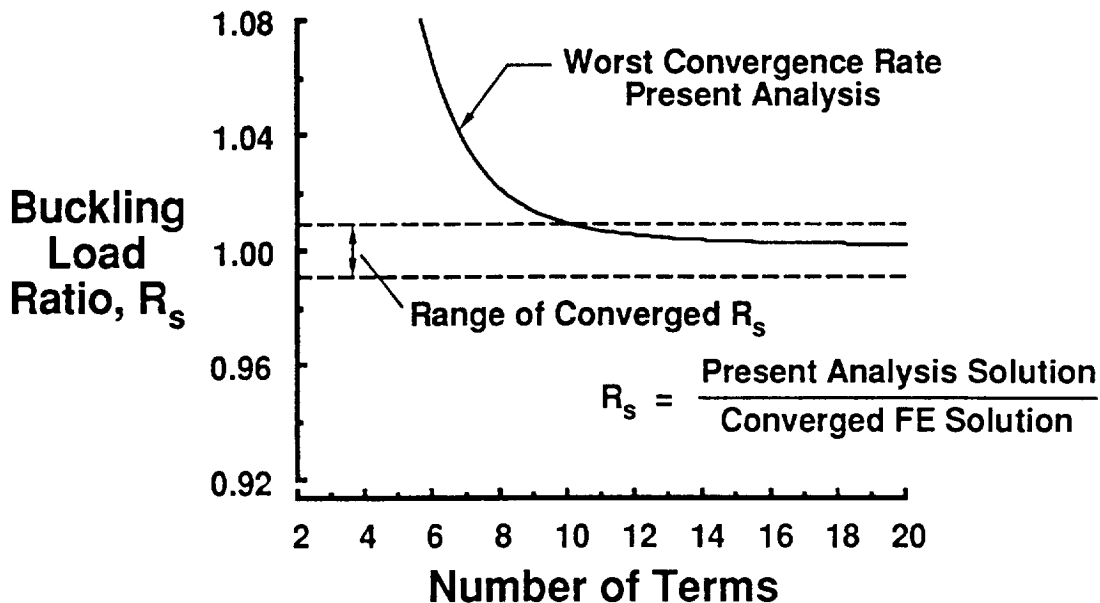


Figure 7

Clamped Panels

Results for the buckling load ratio, R_s , as a function of the number of terms in series solution are shown in figure 8 for plates with clamped boundary conditions. The buckling load ratio is defined as the ratio of the present analysis solution to the converged finite element solution. The finite element solution is assumed to be exact. Buckling load results for the case with the worst convergence rate are shown by the solid line on the figure. For this case, twelve terms for the assumed series solution were required to obtain a converged R_s within eight percent of the exact solution. Most other cases had converged results with much fewer terms for the assumed series solution. All 48 test cases converged to within plus eight to minus three percent of the exact solution. The reason for the slower convergence as compared to the simple support results is that the assumed series for clamped boundaries does not capture the buckling behavior as rapidly as the assumed series for simple support boundaries. The range of converged results for panels with clamped boundaries is wider than the converged results for panels with simple support boundaries. This difference is due to the limitations of the present analysis.

Convergence Rate and Comparison with FE Results

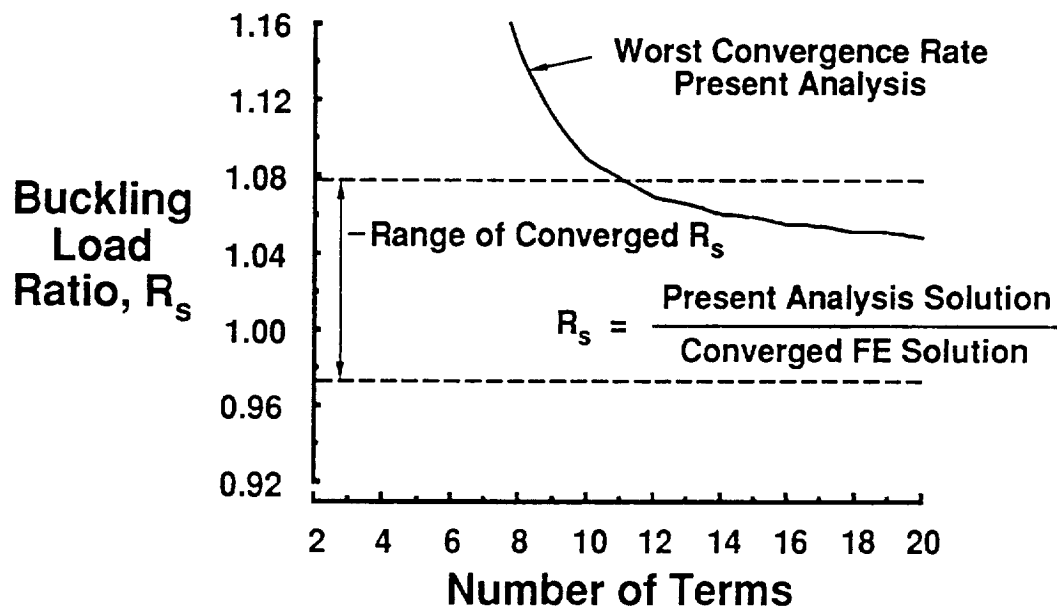


Figure 8

Limitations of Shallow Shell Theory

The theory used in the present work is limited to shallow shells. Results for the buckling load ratio, R_s , as a function of the width-to-radius-of-curvature ratio, b/R , are shown in figure 9. The ratio, b/R , is a measure of the curvature of the shell, e.g., for $b/R = 0$, the panel is a flat plate. Results are shown on the figure for a clamped panel subjected to three types of loading: shear only, compression and shear, and compression only. The material, stacking sequence, and geometry (except for the radius of curvature R) for the panel remain constant. The results on the figure show that the accuracy of R_s decreases as the shell curvature, b/R increases. However, this decrease in accuracy depends on the panel loading. When the panel is loaded in shear only, the accuracy of R_s decreases very slowly as b/R increases. For the case of compression only loading, however, the accuracy of R_s decreases rapidly as b/R increases. The results for combined compression and shear loading are between those for compression only loading and for shear only loading. An example of the application of the present analysis for the conservative case of compression only loading is as follows: a 5 percent error ($R_s = 0.95$) results for a panel with $b/R = 0.22$. This example suggests that the present theory may be used for panels with $b/R < 0.22$ if a 5 percent error is allowable. The results on the figure are typical for the present analysis.

Clamped Panel Example - Comparison with FE Results

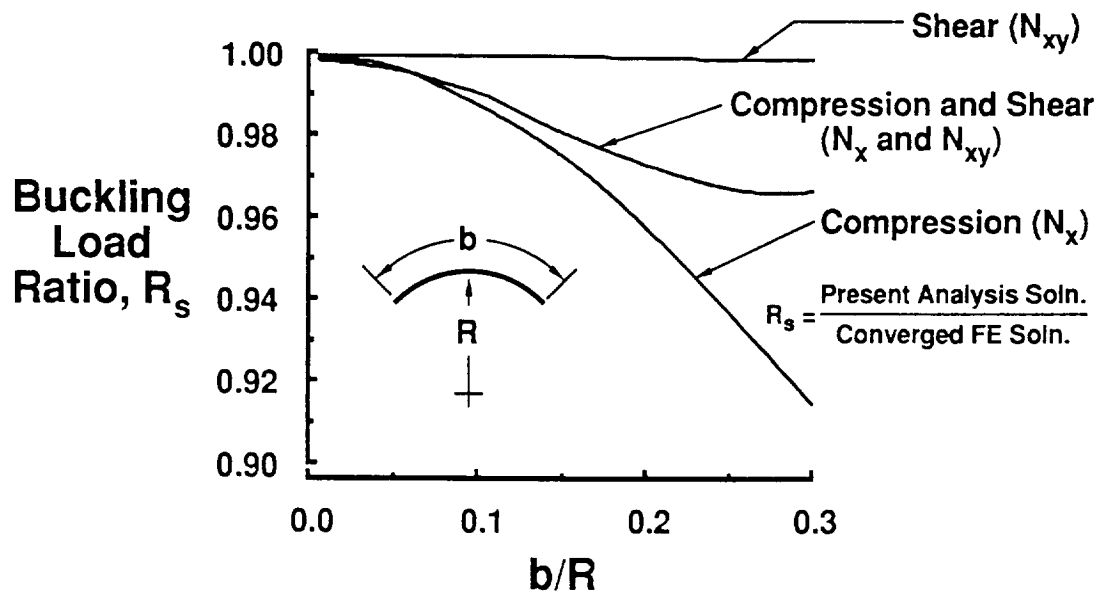


Figure 9

Computational Efficiency

A significant advantage of the present analysis is its computational efficiency. In an optimization program the analysis portion may be performed hundreds or even thousands of times. Thus, the analysis must be as computationally efficient as possible in terms of CPU time. The results presented herein were obtained using a Convex C-240 computer for both the present analysis and the finite element analysis. The FORTRAN programs for the present analysis used the vectorizing option in the compiler. The finite element results were generated with the COMET finite element computer program [4]. The computational efficiency of the present analysis is outlined in figure 10. The present analysis was 340 to 420 times faster and 50 to 80 times faster than the corresponding finite element analysis for panels with simple support boundary conditions or with clamped boundary conditions, respectively. The times required for completing the present analysis suggest that this analysis is well suited for optimization.

- **Simply Supported Analysis**
 - **340 to 420 times faster than finite element analysis**
 - **Ten term solution requires \approx 0.5 to 0.8 CPU seconds**
- **Clamped Analysis**
 - **50 to 80 times faster than finite element analysis**
 - **Ten term solution requires \approx 3.7 to 4.0 CPU seconds**

Present analysis well suited for optimization

Figure 10

Concluding Remarks

A buckling analysis for cylindrically curved composite sandwich panels has been derived and implemented. This analysis is capable of analyzing panels with orthotropic facesheets and first-order transverse shear effects. The panels can be subjected to linearly varying N_x and N_y loads, in addition to a constant N_{xy} load. Both simple support and clamped boundary conditions are included in the analysis.

The governing equations for the analysis are a set of modified Donnell's equations in the unknowns w , Q_x , and Q_y . These equations use inverse differential operators to avoid escalating the partial differential equations. Series solutions which satisfy all boundary conditions are assumed for w , Q_x , and Q_y . A direct application of Galerkin's method is then used to solve the governing equations. Because of assumptions made during the derivation, this analysis is only valid for shallow shells.

To verify the accuracy of the analysis, comparisons were made with results obtained from a finite element analysis. For simply supported panels, the present analysis buckling load is usually within ± 1 percent of the finite element results for shallow shells. For clamped panels the present analysis yields less accurate, but still acceptable, results; the buckling load is within -4 to +8 percent of the finite element results for shallow shells. As the curvature of the panels is increased, and the shell becomes less shallow, the accuracy of the present analysis decreases. The degree to which the accuracy decreases with increasing curvature is a strong function of the loading. Within the context of the shallow shell assumptions, the present analysis provides useful results for a wide variety of structures.

References

1. Cruz, Juan R.: Optimization of Composite Sandwich Cover Panels Subjected to Compressive Loadings. NASA TP-3173, 1991.
2. Stein, Manuel; and Mayers, J.: A Small-Deflection Theory for Curved Sandwich Plates. NACA Report 1008, 1951.
3. Batdorf, S. B.: On the Application of Inverse Differential Operators to the Solution of Cylinder Buckling and Other Problems. Proceedings of the AIAA/ASME 10th Structures, Structural Dynamics and Materials Conference, New Orleans, Louisiana, April 14-16, 1969, pp. 386-391.
4. Lotts, C. G.; Greene, W. H.; McCleary, S. L.; Knight, N. F.; Paulson, S. S.; and Gillian, R. E.: Introduction to the Computational Mechanics Testbed. NASA TM 89096, 1987.